Differentiation of gram-negative intermembrane phospholipid transporter function by fatty acid saturation preference

Ashutosh K. Rai[1], Katsuhiro Sawasato[2], Anastasiia Kozlova[2], Genevieve C. Sparagna[3], Mikhail V. Bogdanov[2], and Angela M. Mitchell[1]*

[1] Department of Biology, Texas A&M University, College Station, Texas, USA

[2] Department of Biochemistry and Molecular Biology, McGovern Medical School at The University of Texas Health Science Center at Houston, Houston, Texas, USA

[3] Department of Medicine, Division of Cardiology, University of Colorado Anschutz Medical Campus, Aurora, Colorado, USA

*Address correspondence to Angela M. Mitchell, amitchell@bio.tamu.edu

Keywords: phospholipid trafficking, gram-negative envelope, outer membrane, lipid metabolism, cold sensitivity

Abstract

The gram-negative outer membrane protects against environmental stress and antibiotics. Phospholipid transport to this membrane is under intense investigation and, in *Escherichia coli*, YhdP, TamB, and YdbH have recently been shown to mediate this transport. However, strains without the main transporters, YhdP and TamB, have different phenotypes, demonstrating distinct functions. We investigated these functions using the synthetic cold sensitivity of a deletion strain of *yhdP* and *fadR*, a fatty acid metabolism regulator. Cold sensitivity is suppressed by Δ*tamB* forcing transport to YdbH and demonstrating TamB dysfunction. Increased cardiolipin and fatty acid saturation are necessary for cold sensitivity and lowering either suppresses the sensitivity. Our data and simulations support a model where YhdP transports more saturated phospholipids and TamB transports more unsaturated phospholipids, allowing independent regulation of inner and outer membrane saturation by altering the YhdP:TamB activity ratio and providing a mechanism for maintaining outer membrane homeostasis under changing conditions.

Introduction

The gram-negative bacterial cell envelope has an outer membrane (OM) that sits outside the aqueous periplasm and peptidoglycan cell wall. The OM provides a barrier against various environmental stresses including toxic molecules such as antibiotics and osmotic pressure[1-6]. Unlike the inner membrane (IM), a phospholipid bilayer, the OM is largely composed of phospholipids in its inner leaflet and LPS (lipopolysaccharide) in its outer leaflet[2,7]. However, both membranes are asymmetric as the IM has different phospholipid composition between its inner and outer leaflets[8]. Outer membrane proteins (OMPs) form a network across the cell surface interspersed with phase separated LPS patches[9]. Lipoproteins are generally anchored in the inner leaflet of the OM[10].

OM components are synthesized in the cytoplasm or IM and transported to the OM. OMP[11], lipoprotein[10], and LPS[12] transport pathways are well defined. However, until recently, intermembrane phospholipid transport (between the IM and OM), especially anterograde transport from the IM to the OM, has remained largely opaque. Phospholipids are synthesized at the IM's inner leaflet[13] and rapid, bidirectional intermembrane phospholipid transport occurs[14], even without ATP[15]. Phospholipid transport has relaxed specificity, allowing transport of non-native lipids[16,17]. However, intermembrane phospholipid composition differences are maintained[18-22]. Establishment and maintenance of this defined lipid topography between the IM and the OM must involve the coordinated biosynthesis and balanced bidirectional trafficking of specific phospholipids across the IM and from the IM to the OM[23].

A recent study has demonstrated anterograde phospholipids transport is mediated by a high-flux, diffusive system in *Escherichia coli*[24]. The Mla system removes mislocalized phospholipids from the OM outer leaflet and returns them to the IM[25]. A gain-of-function allele, *mlaA**[26,27], opens a channel allowing phospholipids to flow from the OM inner to outer leaflet[26,28], resulting in a PldA-mediated increase in LPS production, OM vesiculation, and increased phospholipids flow to the OM[26,27]. When nutrients are depleted, inhibiting phospholipid production, cell lyse due to loss of IM integrity[15,17]. Single cell imaging of *mlaA** cells confirmed IM flows to the OM at a fast rate and loss of YhdP, an inner membrane protein, could significantly slow phospholipid flow to the OM resulting in loss of OM integrity before IM lysis[24], suggesting YhdP might play a role in intermembrane phospholipid transport.

Very recently, YhdP and two homologs, TamB and YdbH, were demonstrated to be intermembrane phospholipid transporters[29,30]. Ruiz, *et al*. investigated AsmA family proteins and found Δ*yhdP* Δ*tamB* mutants showed synthetic OM permeability and stationary phase lysis[29]. Moreover, Δ*yhdP*, Δ*tamB*, and Δ*ydbH* are synthetically lethal and genetic interactions with *mlaA* and *pldA* show involvement in OM phospholipid homeostasis. Predicted structures of YhdP, TamB, and YdbH[31,32], as well as a partial crystal structure of TamB[33], have a β-taco fold domain with a hydrophobic pocket, resembling eukaryotic lipid transporters[34-37]. These data suggest YhdP, TamB, and YdbH are involved in phospholipid transport. Douglass, *et al.* confirmed the synthetic lethality of Δ*yhdP*, Δ*tamB*, and Δ*ydbH* and demonstrated a Δ*tamB* Δ*ydbH* mutant with

reduced *yhdP* expression had decreased OM phospholipids, directly demonstrating involvement in intermembrane phospholipid transport[30].

Nevertheless, why there are three intermembrane phospholipid transport proteins remains unanswered, although it is clear the proteins are not fully redundant. YdbH seems to play a more minor role than YhdP and TamB[29,30] and the screen identifying Δ*yhdP* as slowing *mlaA** lysis did not identify Δ*tamB* or Δ*ydbH*[24]. In addition, we previously identified a role for YhdP in stationary phase SDS (sodium dodecyl sulphate) resistance and modulating cyclic enterobacterial common antigen activity[38,39] not shared by TamB and YdbH (**Fig. S1**)[29,30,38,39].

Here, we investigated the differentiation of YhdP and TamB function and identified synthetic cold sensitivity due to impaired TamB function in a strain with Δ*yhdP* and Δ*fadR*, a transcriptional regulator of fatty acid biosynthesis and degradation acting as a switch between these pathways in response to acyl-CoA[40]. FadR is necessary for normal levels of unsaturated fatty acids to be synthesized[41]. The Δ*yhdP* Δ*fadR* mutant has increased levels of a specific phospholipid, cardiolipin, and decreasing cardiolipin suppresses cold sensitivity. Furthermore, increasing unsaturated fatty acids levels suppresses. Overall, our data lead us to a model where TamB and YhdP functions are differentiated based on phospholipid fatty acid saturation state, with TamB transporting more unsaturated phospholipids and YhdP transporting more saturated phospholipids. This model is supported by computational data suggesting phospholipids can stall phospholipids near the center of TamB, which would impair diffusive flow of stiff, saturated phospholipids.

Results

Loss of FadR and YhdP results in cold sensitivity due to impaired TamB function. To investigate YhdP-TamB function differentiation, we created a Δ*yhdP* Δ*fadR* strain. A Δ*fadR* strain is expect to have decreased fatty acid synthesis, increased fatty acid degradation, and increased fatty acid saturation[40,41]. Δ*yhdP* Δ*fadR* cultures grown at 30 °C lagged for more than 8 hours, followed by highly variable growth, suggesting suppressor outgrowth (**Fig.1A**). The growth defect was decreased at 37 °C and completely absent at 42 °C. To confirm this cold sensitivity, we performed efficiency of plating assays (EOPs) and demonstrated severe cold sensitivity in the Δ*yhdP* Δ*fadR* strain (5 logs at 30 °C and 3 logs at 37 °C) (**Fig. 1B**). Cyclic enterobacterial common antigen is necessary for Δ*yhdP*'s OM permeability phenotypes[39]. However, the Δ*yhdP* Δ*fadR* strain's cold sensitivity was unchanged when enterobacterial common antigen was removed (Δ*wecA*)[42] (**Fig. 1C**).

Given their role in phospholipid transport, we expected Δ*tamB* and/or Δ*ydbH* to show similar synthetic phenotypes with Δ*fadR*; however, Δ*fadR* Δ*tamB* and Δ*fadR* Δ*ydbH* strains had no growth defects (**Fig 1D**). We, therefore, hypothesized the Δ*yhdP* Δ*fadR* cold sensitivity was due to impairment of another phospholipid transporter(s). Δ*ydbH* in the Δ*yhdP* Δ*fadR* strain did not alter cold sensitivity (**Fig. 1E**). However, Δ*tamB* in the Δ*yhdP* Δ*fadR* background completely

118 suppressed the cold sensitivity (**Fig. 1F**). Consistent with previous observations[29], the Δ*yhdP*
119 Δ*fadR* Δ*tamB* strain was mucoid due to Rcs stress response activation and colanic acid capsule
120 production. Deleting *rcsB*, a Rcs response regulator, prevented mucoidy but did not affect
121 suppression (**Fig. 1F**). We observed only minimal growth phenotypes in the Δ*yhdP* Δ*fadR* Δ*tamB*
122 strain, similar to those of Δ*tamB* and less severe than those of Δ*fadR* (**Fig. 1G**), eliminating slow
123 growth as a suppression mechanism. Together, these data demonstrate suppression from loss
124 of TamB is due to reprieve of impaired TamB function, shifting phospholipid transport to YdbH.

125 We next looked for envelope homeostasis alterations in the Δ*yhdP* Δ*fadR* strain with TamB
126 impairment. To identify lysis and/or severe OM permeability defects at 30 °C, we assayed CPRG
127 (chlorophenol red-β-D-galactopyranoside) processing. CPRG must contact LacZ in the cytoplasm
128 or supernatant to release chlorophenol red[43]. Compared to wild type or single mutants, the Δ*yhdP*
129 Δ*fadR* strain had increased CPRG processing (**Fig. S2A**), demonstrating lysis or increased
130 envelope permeability. When we assayed resistance to molecules excluded by the OM[1,38,39,44,45]
131 at 37 °C, a semi-permissive temperature, the Δ*yhdP* Δ*fadR* strain showed sensitivity to
132 vancomycin, a large scaffold antibiotic, and SDS EDTA compared to single mutants (**Fig. S2B**).
133 However, with bacitracin treatment or EDTA treatment alone, the Δ*yhdP* Δ*fadR* strain
134 phenocopied the Δ*fadR* single deletion (**Fig. S2CD**). LPS levels were not altered in the Δ*yhdP*,
135 Δ*fadR*, or the Δ*yhdP* Δ*fadR* strain (**Fig. S2E**). OM asymmetry mutations (i.e., Δ*pldA*, Δ*mlaA*)[25-27,46]
136 did not have suppressive or synthetic effects on cold sensitivity in the Δ*yhdP* Δ*fadR* strain (**Fig.
137 S3AB**), suggesting against a causal loss of OM asymmetry. Overall, the changes in OM
138 permeability did not seem sufficient to cause lethality at lower temperature, suggesting the
139 phospholipid transport disruption affects both IM and OM integrity.

140 **Increased cardiolipin is necessary for impaired TamB function.** We investigated phospholipid
141 composition of the wild-type and Δ*yhdP* Δ*fadR* strains grown at the permissive temperature (42
142 °C) and grown to early log phase at 42 °C, then downshifted to 30 °C. *E. coli* phospholipid
143 composition is generally 75% phosphatidylethanolamine (PE), 20% phosphatidylglycerol (PG),
144 and 5% cardiolipin (CL) with CL increasing in stationary phase[13,47]. Of the three CL synthases,
145 ClsA and ClsB synthesizes CL from two PG molecules, while ClsC synthesizes CL from one PG
146 and one PE molecule, so CL and PG levels are generally reciprocally regulated[48-51]. For both
147 strains and conditions, the levels of PE were similar (**Fig. 2A**). However, the Δ*yhdP* Δ*fadR* strain
148 had increased CL and concomitant decreased PG compared to the wild-type strain, especially at
149 30 °C. PgsA synthesizes phosphatidylglycerol-phosphate and is the first enzyme differentiating
150 PG and PE biosynthesis. PgsA depletion would decrease both PG and CL levels, reversing
151 increased CL levels and exacerbating decreased PG levels in the Δ*yhdP* Δ*fadR* strain. We tested
152 the PgsA depletion in a strain background (Δ*rcsF* Δ*lpp*) where *pgsA* is non-essential[52-55]. When
153 *pgsA* expression was induced (arabinose panel), the Δ*yhdP* Δ*fadR* PgsA-depletion strain had
154 equal cold sensitivity to the Δ*yhdP* Δ*fadR* strain (**Fig. 2B**). When *pgsA* expression was repressed
155 (glucose panel), the Δ*yhdP* Δ*fadR* cold sensitivity was partial suppressed, suggesting increased
156 CL, and not decreased PG, may be necessary for cold sensitivity. A Δ*yhdP* Δ*fadR* strain with all
157 cardiolipin syntheses removed (Δ*clsABC*) or with the main exponential phase cardiolipin synthase
158 removed (Δ*clsA*) had undetectable CL levels (**Fig. 2A**) and was completely suppressed for cold

159 sensitivity (**Fig. 2CD**). Δ*clsB or* Δ*clsC* caused a smaller decrease in CL levels that was very similar
160 between the two strains (11% to 7.4% vs. 7.6%, respectively) (**Fig. 2A**). Surprisingly, Δ*clsC*
161 completely suppressed the cold sensitivity, while Δ*clsB* did not (**Fig. 2EF**). Thus, increased CL is
162 necessary for impaired TamB function leading to cold sensitivity but CL levels alone cannot
163 explain the phenotype: another factor, such as a specific form or localization of CL, is required.

164 **Increased *fabA* expression suppresses cold sensitivity.** To identify other factors involved in
165 the cold sensitivity, we applied a forward genetic approach by isolating spontaneous suppressor
166 mutants capable of growing at 30 °C and identified a suppressor mutant (Suppressor 1) that
167 restored growth at 30 °C (**Fig. 3A**), decreased CPRG processing (**Fig. S2A**), and had very similar
168 CL to the Δ*yhdP* Δ*fadR* strain (**Fig. 3B**, **Fig. S4**). We identified a point mutation in the *fabA*
169 promoter region in Suppressor 1 (**Fig. 3C**) and confirmed this mutation was sufficient for
170 suppression (**Fig. 3D**). FabA is a dehydratase/isomerase that introduces *cis* unsaturation into fatty
171 acids[13,56] and *fabA* is expressed from two promoters controlled by FadR and FabR[57,58]. FadR
172 activates *fabA* expression, while FabR represses. Thus, *fadR* deletion would be expected to lower
173 *fabA* expression. The suppressor mutation was located in the *fabA* promoter FabR binding site
174 (**Fig. 3C**) and we hypothesized this mutation would increase *fabA* expression. *fabA* mRNA levels
175 were more than 4-fold lower in the Δ*yhdP* Δ*fadR* strain than the wild-type strain (**Fig. 3E**). While
176 lower than wild type, the suppressor mutant increased *fabA* mRNA 1.6-fold over the Δ*yhdP* Δ*fadR*
177 strain.

178 We constructed luciferase reporter plasmids with the wild-type *fabA* promoter region or the *fabA*
179 promoter region containing the suppressor mutation. The reporter with the mutated promoter had
180 higher activity in a wild-type, Δ*fadR,* and Δ*fabR* background (**Fig. 3F**). *fabA* transcription occurs
181 from a promoter downstream of the FabR binding site[58-60]. However, when FadR is removed,
182 transcription moves to the FabR-regulated promoter within the FabR binding region[58-60]. Our data
183 indicate the Suppressor 1 mutation regulates this promoter's constitutive activity rather than FabR
184 binding. To confirm the effect of changing the second promoter's activity, we tested the effect of
185 Δ*fabR* on cold sensitivity in the Δ*yhdP* Δ*fadR* strain and observed partial suppression (**Fig. S5**).
186 The smaller effect of Δ*fabR* compared to Suppressor 1 may result from other gene expression
187 changes or to the smaller relative effect of Δ*fabR* on *fabA* expression (**Fig. 3F**). Overall, these
188 data demonstrate increasing *fabA* expression, which is necessary for unsaturated fatty acid
189 biosynthesis, can relieve TamB impairment in the Δ*yhdP* Δ*fadR* strain without changing CL levels.

190 **Increasing unsaturated fatty acids relieves impaired TamB function.** Given the effect of *fabA*
191 expression on the Δ*yhdP* Δ*fadR* cold sensitivity, we used liquid chromatography-electrospray
192 ionization mass spectrometry (LC/MS) to characterize the strains' phospholipid saturation state
193 (**Dataset S1**, **Fig. 4A-C, Fig. S6**). We analyzed whole cell and IM extracts (**Fig. S6A**) from cells
194 grown to early log phase at 42 °C then downshifted to 30 °C. In whole cell extracts, Δ*fadR* caused
195 increased fully saturated and monounsaturated PE with a concomitant decrease of diunsaturated
196 PE (**Fig. 4A**, **Fig. S6B**). Levels of fully saturated PG were increased with a decrease in mono-
197 and diunsaturated species (**Fig. 4B**, **Fig. S6C**). The Δ*fadR* strain demonstrated increased
198 monounsaturated CL with a concomitant decrease in triunsaturated CL (**Fig. 4C**, **Fig. S6D**).

199 Compared to the Δ*fadR* strain, the Δ*yhdP* Δ*fadR* strain had slightly increased saturation for all
200 three phospholipids, with the largest increase in fully saturated PE. Suppressor 1 demonstrated
201 decreased saturation of all three phospholipids but especially of PE compared to the Δ*yhdP* Δ*fadR*
202 strain (**Fig. 4A-C**, **Fig. S6E-G**). The OM is enriched for PE and its saturated species compared to
203 the IM outer leaflet[8,19-22] making the large PE changes intriguing. We wondered whether the
204 suppression difference between Δ*clsC* and Δ*clsB* resulted from the CL saturation state. However,
205 The Δ*yhdP* Δ*fadR* Δ*clsB* and Δ*yhdP* Δ*fadR* Δ*clsC* strains had very similar CL profiles (**Fig. 4C**,
206 **Fig. S6G**), suggesting another qualitative difference affecting suppression, perhaps CL
207 localization.

208 We hypothesized increasing unsaturated fatty acids suppresses Δ*yhdP* Δ*fadR* cold sensitivity and
209 performed EOPs for cold sensitivity on media containing an unsaturated fatty acid (oleic acid,
210 C18:1 *cis*-9). Oleic acid addition suppressed the Δ*yhdP* Δ*fadR* strain's cold sensitivity (**Fig. 4D**).
211 Supplementing oleic acid increases unsaturated phospholipids and provides an exogenous fatty
212 acid source. To differentiate between saturation state and fatty acid availability, we compared
213 treatment with oleic acid and saturated stearic acid (C18:0). Only oleic acid, and not stearic acid,
214 suppressed the Δ*yhdP* Δ*fadR* strain's cold sensitivity (**Fig. 4E**), confirming increasing unsaturated
215 fatty acids, not fatty acid availability suppresses.

216 These data suggested the Δ*yhdP* Δ*fadR* strain was impaired in intermembrane transport of more
217 saturated phospholipids. To investigate phospholipid transport defects, we compared
218 phospholipids in whole cell and IM extracts (**Fig. S6A**). OM extracts are generally contaminated
219 with IM, complicating interpretation. PG and CL showed small differences between whole cell and
220 IM extracts but were largely similar between strains (**Fig. 4BC**). However, PE showed larger strain
221 differences. In the wild-type strain, fully saturated PE was enriched in whole cells compared to
222 IM, demonstrating increased OM saturated PE (**Fig. 4A**, **Fig. S6H**). In the Δ*fadR* strain, whole
223 cell and IM extracts had similar fully saturated PE levels, but IM extracts had higher diunsaturated
224 PE, still suggesting OM enrichment of more saturated PE. However, in the Δ*yhdP* Δ*fadR* strain,
225 while the IM had higher levels of diunsaturated PE, the IM was underrepresented for fully
226 saturated PE (**Fig. 4A**, **Fig. S6H**). The Δ*yhdP* Δ*fadR* IM also had much lower short chain PE
227 levels (30:0 and 30:1) than whole cells (**Fig. 4A**, **Fig. S6HI**). Short chain phospholipids decrease
228 membrane rigidity and remain fluid at lower temperatures[61]. Thus, the short fatty acid PE increase
229 after short-term adaptation to 30 °C may be an attempt to increase fluidity and restore balance
230 between the membranes. In Suppressor 1, the profile more closely resembled Δ*fadR* cells. Thus,
231 the alteration of PE saturation and fatty acid length in the Δ*yhdP* Δ*fadR* OM demonstrates a
232 disruption in intermembrane phospholipid trafficking due to impairment of TamB function.

233 **Suppression causes fatty acid metabolism and stress response alterations.** In wild-type
234 cells, *fabA* overexpression does not change saturation: FabB is rate limiting for unsaturated fatty
235 acid biosynthesis[62]. We were intrigued Suppressor 1 altered saturation without directly effecting
236 *fabB* expression. We also wondered if CL levels in the Δ*yhdP* Δ*fadR* strain are transcriptionally
237 regulated. Thus, we investigated the transcriptional landscape of the wild type, the Δ*yhdP* Δ*fadR*,
238 and Suppressor 1 strains after a 30 minute downshift to 30 °C to determine: (i) whether the Δ*yhdP*

239 Δ*fadR* strain had altered *cls* gene expression; (ii) whether Suppressor 1 had other transcriptional
240 changes; and (iii) why increased *fabA* expression decreased saturation. All differentially
241 expressed genes (>2-fold change, $p<0.05$) are listed in **Dataset S2**. Principle component analysis
242 of these genes showed the closest relation between Δ*yhdP* Δ*fadR* strain and Suppressor 1, while
243 the wild-type strain was more distantly related (**Fig. 5A**, **S7A**). Nevertheless, Suppressor 1 was
244 more closely related to wild type than was the Δ*yhdP* Δ*fadR* strain. Most differentially regulated
245 genes between Δ*yhdP* Δ*fadR* and wild type and Suppressor 1 and wild type were upregulated
246 (**Fig. 5BC**, **S7BC**). Many of the most highly regulated genes are FadR-regulon members. The
247 majority of differentially regulated genes in Suppressor 1 compared to Δ*yhdP* Δ*fadR* are
248 downregulated (**Fig. 5D, S7D**). These genes are involved in many cellular pathways and likely
249 reflect the decreased cellular stress (**Table S2**). Indeed, many external stress response genes
250 are more enriched in Δ*yhdP* Δ*fadR* than in Suppressor 1 (**Fig. S8A**).

251 No significant expression changes occurred in the CL biosynthesis pathway (**Fig. 5E**) or other
252 phospholipid biosynthesis genes (**Fig. S8B**). The increased cardiolipin in Δ*yhdP* Δ*fadR* and
253 Suppressor 1 may be post-transcriptional or due to a change in a regulatory pathway not yet
254 altered after 30 minutes at 30 °C (**Fig. S8C**). We examined the expression of genes in fatty acid
255 synthesis and degradation, many of which are members of the FadR regulon. In Δ*yhdP* Δ*fadR*
256 compared to wild type, many fatty acid biosynthesis genes significantly decreased while many
257 fatty acid degradation genes significantly increased (**Fig. 5F**), consistent with Δ*fadR* effects. While
258 *fabA* expression is decreased, *fabB* expression is not changed, explaining why increased *fabA*
259 expression causes decreased saturation in Suppressor 1.

260 **TamB modeling shows potential for blocking interactions.** Our data demonstrate the Δ*yhdP*
261 Δ*fadR* strain's cold sensitivity is due to impaired TamB function, and increased phospholipid
262 saturation and cardiolipin are necessary for impairment. We hypothesized TamB has a substrate
263 preference and TamB impairment is due to "clogging" by inappropriate substrates. As the OM is
264 enriched for PE[8,19-22], we modeled docking of a short-chain saturated PE (14:0, 14:0) with the
265 AlphaFold predicted structures of YhdP, TamB, and YdbH[31,32]. A partial TamB crystal structure
266 has a similar conformation to the predicted structures with a long, hydrophobic groove formed by
267 β-sheets[33]. When docking with YhdP and YdbH (**Fig. 6AB**), the short-chain, saturated PE showed
268 sites, generally binding one PE conformation, spread throughout the hydrophobic cavity[29,33].
269 Contrarily, when docking with TamB, several binding sites interacted with PE molecules in many
270 possible conformations (**Fig. 6C**). When we modeled transit of PE through TamB, the molecule
271 became "trapped" in the center, curved portion of TamB, sampling many possible binding sites
272 and conformations (**Movie S1**). Other PE and PG molecules with differing saturations states
273 showed similar binding patterns for the three proteins (**Fig. S9**). Together with our genetic and
274 biochemical data, these data suggest more hydrophobic and rigid saturated phospholipids could
275 interact improperly with TamB and impair diffusive phospholipids flow.
276
277

Discussion

The identification of YhdP, TamB, and YdbH as intermembrane phospholipid transporters[29,30] posed the tantalizing question: why is having three transporters advantageous? Here, we demonstrate each protein plays a distinguishable role in phospholipid transport that can be differentiated based on genetic interactions with lipid metabolism. Disruption of FadR and YhdP function causes synthetic cold sensitivity not shared by TamB or YdbH, due to impaired TamB function, which can be suppressed by forcing transport to YdbH. This phenotype requires both increased CL and saturated fatty acids, and decreasing either suppresses. In addition, our data demonstrate CL synthesized by ClsB and ClsC is qualitatively different—resulting in differential suppression phenotypes—likely due to differences in CL localization and localized membrane fluidity[63] or TamB interaction. Molecular docking simulations suggest TamB has different interactions with phospholipids than the other transporters likely making transport of unsaturated phospholipids unfavorable.

In our model based on these data (**Fig. 6D-F**), the functions of YhdP and TamB are diversified based on the saturation of the phospholipids they transport: YhdP transports mainly phospholipids with more saturated fatty acids, while TamB transports phospholipids with more unsaturated fatty acids (**Fig. 6D**). Our data and previous data[29,30] agree YdbH plays a relatively minor role. In the Δ*yhdP* Δ*fadR* strain, YhdP's absence forces more saturated phospholipids to be transported by TamB. At 30 °C, where CL levels are high and membrane fluidity is decreased, our simulations suggest TamB becomes "clogged" by phospholipids cycling in the curved region of the protein, impeding transport (**Fig. 6E**). CL could contribute by failing to move around cycling phospholipids or by locally decreasing fluidity. Impaired transport explains the difference in OM PE saturation profiles between the Δ*yhdP* Δ*fadR* strain and the other, non-cold-sensitive strains. When Δ*tamB* is deleted, phospholipid flow is forced to YdbH, preventing clogging and relieving cold sensitivity (**Fig. 6F**). YdbH's ability to successfully transport phospholipids in the Δ*yhdP* Δ*tamB* strain only when TamB is absent may be because YhdP and TamB are preferred transporters (e.g., preferred interaction partners for other pathway members), due to direct toxicity caused by TamB clogging, or because *ydbH* is upregulated.

Although both fatty acid saturation and high CL levels are required for the Δ*yhdP* Δ*fadR* strain's cold sensitivity, two lines of evidence point to saturation rather than headgroup as the factor separating YhdP and TamB function. (i) YhdP loss slows phospholipid transport from the IM to the OM in a *mlaA** mutant, which losses OM material due to vesiculation and lysis when phospholipid biosynthesis is insufficient to replace lost phospholipids[24,26]. CL only accounts for 5% of phospholipids in exponentially growing cells making unlikely loss of CL transport could slow net phospholipid transport to the extent required to slow lysis. (ii) Δ*tamB* has a small growth defect at 30 °C (**Fig. 1G**) not observed at higher temperature[29,30], perhaps due to increased unsaturated phospholipids[64-66] resulting in decreased net OM transport by YhdP or to lower OM fluidity. Together, these observations provide strong evidence YhdP has a substrate preference for phospholipids with more saturated fatty acids, while TamB prefers phospholipids with more unsaturated fatty acids.

318 Our model suggests the IM and OM saturation state could be independently regulated based on
319 YhdP and TamB activity or levels. IM saturation is regulated by altering the composition of newly
320 synthesized fatty acids, while OM saturation could be separately regulated by allowing increased
321 transport of more saturated or unsaturated phospholipids as necessary. IM and OM saturation
322 has been studied in several strains of *E. coli* and in *Yersinia pseudotuberculosis*[18-21] and higher
323 saturated fatty acid levels were observed in the OM than in the IM, supporting discrimination of
324 phospholipids transport based on saturation. The IM needs to maintain an appropriate level of
325 fluidity to allow IM proteins to fold and diffuse, to allow diffusion of hydrophobic molecules, to
326 regulate cellular respiration, and to maintain membrane integrity[67,68]. However, the OM is a
327 permeability barrier, a load-bearing element that resists turgor pressure[1-6], and has an outer leaflet
328 consisting of LPS[2,7]. LPS has saturated acyl chains and is largely immobile in *E. coli*[69] and a
329 specific phospholipid saturation level may be necessary to match or counterbalance LPS rigidity.
330 OM phospholipids may also play a role in the physical strength of the membrane. Interestingly,
331 previous work has demonstrated that the tensile strength of the OM is lessened in a *yhdP*
332 mutant[24].

333 Possessing two different phospholipid transporters with different saturation state preferences
334 would allow the cell to adapt OM saturation to changing conditions including temperature shifts,
335 chemical insults, or changes synthesis of other OM components (e.g., LPS or OMPs). A recent
336 study demonstrated in *Y. pseudotuberculosis* the difference in saturation levels between the
337 membranes is exaggerated at 37 °C compared to 8 °C[21]. Thus, conditions where IM and OM
338 saturation are independently regulated exist and this regulation is likely important for optimum
339 fitness of the cells. Transcriptional regulation of *yhdP* and *tamB* has not been thoroughly explored.
340 It seems likely *yhdP* transcription is quite complex with several promoters and transcriptional
341 termination sites[70-72]. *tamB* is predicted to be in an operon with *tamA* (which codes for an OMP
342 necessary for TamB function) and *ytfP*[70,73] and to have a σ^E-dependent promoter[74]. The σ^E stress
343 response is activated by unfolded OMP accumulation, and downregulates the production of OMPs
344 and upregulates chaperones and folding machinery[75]. It is intriguing to speculate a change in OM
345 phospholipid composition might aid in OMP folding due to altered biophysical properties and/or
346 lipoprotein diffusion.

347 The mechanism of phospholipid transfer between the IM and OM has been one of the largest
348 remaining questions in gram-negative envelope biogenesis and has remained an area of intense
349 investigation for decades. Recent work has begun to elucidate this pathway by identifying YhdP,
350 TamB, and YdbH as proteins capable of transporting phospholipids between the
351 membranes[24,29,30] . Our work has now clarified that YhdP and TamB have separate roles in
352 phospholipid transport that are differentiated by their preference for phospholipid saturation
353 states. Homologs of YhdP and TamB are found throughout *Enterobacterales* and more distantly
354 related members of the ASMA family are wide spread in gram-negative bacteria[76]. Furthermore,
355 structural predictions of YhdP and TamB are strikingly similar between species[31,32]. Given this, it
356 is quite likely similar mechanisms of discrimination in phospholipid transfer exist in other species.
357 The data we present here provide a framework for investigation of phospholipid transfer and
358 mechanisms differentiating phospholipid transporter function in these species.

359
360
361 **Methods**

362 **Bacterial strains and Growth Conditions. Table S3** lists the strains used in this study. Most
363 knockout strains were constructed with Keio collection alleles using P1vir transduction[77,78]. New
364 alleles were constructed through λ-red recombineering[79], using the primers indicated in **Table S4**.
365 The FLP recombinase-FRT system was used to remove antibiotic resistance cassettes as has
366 been described[79]. *E. coli* cultures were grown in LB Lennox media at 42°C, unless otherwise
367 mentioned. Where noted, LB was supplemented with vancomycin (Gold Biotechnology),
368 bacitracin (Gold Biotechnology), SDS (Thermo Fisher Scientific), EDTA (Thermo Fisher
369 Scientific), oleic acid (Sigma Aldrich), stearic acid (Sigma Aldrich), arabinose (Gold
370 Biotechnology), or glucose (Thermo Scientific). For plasmid maintenance, media was
371 supplemented with 25 µg/mL kanamycin (Gold Biotechnology), 10 or 20 µg/mL chloramphenicol
372 (Gold Biotechnology), or 10 µg/mL tetracycline (Gold Biotechnology) as appropriate.

373 **Plasmid construction.** The pJW15-P_{fabA}, and pJW15-P_{fabA}(-19G>A) reporter plasmids were
374 constructed by amplifying the region upstream of *fabA* from -432 bp to +27 bp relative to the
375 annotated transcriptional start site from wild-type MG1655 or Suppressor 1, respectively, using
376 the Overlap-pJW15-*fabA* FP and RP primers (**Table S4**). pJW15 was amplified using primers
377 Overlap-pJW15-*fabA* FP1 and RP1. The pJW15 plasmid was a kind of gift from Dr. Tracy Raivio
378 (Univeristy of Alberta)[80,81]. The resulting fragments were assembled using HiFi Assembly master
379 mix (New England Biolabs) as per the manufacturer's instructions.

380 **Growth and Sensitivity Assays.** For EOPs assays, cultures were grown overnight, serially
381 diluted, and plated on the indicated media. For *pgsA* depletion, overnight cultures grown in
382 arabinose were washed and diluted 1:100 into fresh LB with 0.2% glucose or arabinose as
383 indicated and grown to OD_{600}=1 before diluting and plating on media with glucose or arabinose
384 respective, as above. EOPs were incubated at 30 °C unless otherwise indicated. Growth curves
385 were performed at the indicated temperature as has been described[39]. For CPRG assays[43],
386 strains were streaked on LB plates supplemented with CPRG (40µg/ml) and IPTG (100 µM)
387 incubated overnight at 30°C.

388 **Suppressor isolation and sequencing.** Serially diluted cultures were spread on LB plates and
389 incubated overnight at a 30°C. Colonies that grew at 30°C were isolated and rechecked for cold-
390 resistance through EOP and growth curves. The suppressors were subjected to whole-genome
391 sequencing to identify potential suppressor mutations. Genomic DNA was isolated from the parent
392 and suppressors using a DNeasy Blood and Tissue Kit (Qiagen) as per the manufacturer's
393 instructions. Library preparation and Illumina sequencing were performed by the Microbial
394 Genome Sequencing Center (MiGS, Pittsburgh, PA, USA). Briefly, Illumina libraries were
395 prepared and the libraries were sequenced with paired-end 151 bp reads on a NextSeq 2000
396 platform to a read depth of at least 200 Mbp. To identify variants from the reference genome
397 (GenBank: U00096.3), reads were trimmed to remove adaptors and the *breseq* software (version

398 0.35.4) was used to call variants[82]. Identified mutations were confirmed with Sanger sequencing.
399 The consensus motif of the FabR binding site of *fabA* was determined using Multiple Em for Motif
400 Elicitation (MEME) tool in the MEME Suite based on the sequence of putative FabR binding sites
401 reported by Feng and Cronan (2011)[57,83,84]. The ability of the identified P_{fabA} mutation to suppress
402 was confirmed by linking the mutant to *zcb*-3059::Tn*10*[85] and transducing to a clean background.

403 **Lux reporter assays.** Overnight cultures of strains harboring the pJW15-P_{fabA} and pJW15-P_{fabA}(-
404 19G>A) plasmids were sub-cultured at (1:100) into 200 µl of fresh LB broth in a black 96-well
405 plate. The plate was incubated in a BioTek Synergy H1 plate reader and the OD_{600} and
406 luminescence intensity were recorded every 2.5 min for 6 hours as described in previously[81,86].
407 Each biological replicate was performed in technical triplicate.

408 **RNA-seq.** Overnight cultures grown at 42°C were subcultured 1:100 into fresh media and
409 incubated at 42 °C until an OD_{600} of 0.4. Then, the cultures were shifted to a 30 °C water bath for
410 30 minutes. 500 µL of each culture was immediately fixed in the RNAprotect Bacteria Reagent
411 (Qiagen) as per the manufacturer's instructions. RNA was purified using the RNeasy Kit (Qiagen)
412 with on-column DNase digestion following the manufacturer's protocol for gram-negative bacteria.
413 Library preparation, Illumina sequencing, and analysis of differentially expressed genes were
414 performed by MiGS. Briefly, samples were treated with RNase free DNase (Invitrogen) and library
415 preparation was performed with the Stranded Total RNA Prep Ligation with Ribo-Zero Plus Kit
416 (Illumina). Libraries were sequenced with 2x50 bp reads on a NextSeq2000 (Illumina).
417 Demultiplexing, quality control, and adapter trimming carried out using bcl-convert (Illumina,
418 v3.9.3) and bcl2fastq (Illumina). Read mapping and read quantification were performed with
419 HISAT2[87] and the featureCounts tool in Subreader[88], respectively. Descriptive statistics of the
420 RNA-seq read data can be found in **Table S1**. The raw RNA-seq data is available in the Sequence
421 Read Archive database (SRA) (https://www.ncbi.nlm.nih.gov/sra, BioProject ID PRJNA965821).
422

423 Raw read counts were normalized using the Trimmed Mean of M values algorithm in edgeR[89] and
424 converted to counts per million. The Quasi-Linear F-Test function of edgeR was used for
425 differential expression analysis. Normalized read values and for all genes as well as differential
426 expression analysis statistics can be found in **Dataset S3**. KEGG pathway analysis was
427 conducted using the *"kegga"* function of limma[90]. Expression of genes differentially expressed
428 (greater than 2-fold change and $p<0.05$) was subjected to principle component analysis, and
429 pathway and enrichment analysis using the EcoCyc Omics Dashboard[90].

430 **Lipid extraction and TLC.** For thin layer chromatography (TLC) experiments, cultures were
431 grown in LB with 1 mCi/mL ^{32}P until OD_{600} of 0.6-0.8 at the indicated temperature. For temperature
432 downshift experiments, cells were grown at 42 ºC until OD_{600} of 0.2 and then transferred to 30 ºC
433 for 2 hours. For lipid extraction, cells were pelleted and resuspended in 0.2 mL of 0.5 M NaCl in
434 0.1 N HCl. Lipids were extracted by first adding 0.6 mL of chloroform:methanol (1:2) to create a
435 single-phase solution. After vigorous vortexing for 30 minutes, 0.2 mL of 0.5 M NaCl in 0.1 N HCl
436 was added to convert the single-phase solution to a two-phase solution. After centrifugation at 20

437 000 x g for 5 minutes at room temperature, the lower phase was recovered and used for TLC.
438 Approximately 2,000 cpm of phospholipid extract was subjected to TLC analysis using a HPTLC
439 60 plate (EMD, Gibbstown, NJ)) developed with either solvent 1: chloroform/methanol/acetic acid
440 [60/25/10 (vol/vol/vol) in **Fig. 2A** or by solvent 2: chloroform/methanol/ammonia/water
441 [65/37.5/3/1] (vol/vol/vol/vol) in **Fig. S4**. Radiolabeled lipids were visualized and quantified using
442 a Phosphoimager Typhoon FLA 9500 (GE). Images were processed and quantified using
443 ImageQuant™ software for scanning and analysis. The phospholipid content is expressed as
444 molecular percentage of the total phospholipids (correcting for the two phosphates per molecule
445 of CL).

446 **Phospholipid composition analysis.** Whole cell lipid extracts were isolated as for TLC
447 temperature downshift experiments without radiolabelling. IMs were isolated and extracts were
448 prepared as has been previously described[91]. Briefly, cells from temperature downshifted cultures
449 were lysed using a French press at 8,000 psi and whole cells were pelleted by centrifugation at
450 30 000 x g for 20 minutes. Then, the supernatant was centrifuged at 150 000 x g for 1 hour. The
451 resulting pellet contained pure IM as demonstrated by immunoblot analysis (**Fig. S6A**). Relative
452 amounts of CL, PG, and PE were determined in these lipid extracts using liquid chromatography
453 coupled to electrospray ionization mass spectrometry (LC/MS) in an API 4000 mass spectrometer
454 (Sciex, Framingham, MA, USA) using normal phase solvents as previously published[92]. Individual
455 molecular species of CL, PG, and PE were expressed as a percentage within their individual
456 phospholipid by summing all the species and dividing by that sum for each phospholipid. The
457 identities of CL species were confirmed using tandem mass spectrometry.

458 **Molecular Docking Simulations.** Predicted protein structures were accessed from the
459 AlphaFold Database[31,32]. To sample phospholipid ligand conformations along the predicted
460 protein structures, molecular docking simulations were perfomed using the AutoDock Program[93].
461 Structures were converted from PDB to PDBQT format for ligands and proteins using the Open
462 Babel ToolBox[94] and the MGLTtools software (available from ccsb.scripps.edu/mgltools),
463 respectively. The 3D search field for molecular docking was split into smaller fields with a size
464 less than 30 cubic Å, overlapping by 20 Å. Search fields were considered valid if they contained
465 at least three surface exposed amino acid. Docking results from smaller fields were merged into
466 one complete search field. Selection of the most probably ligand conformations was carried out
467 by the convergence method calculated by the RMSD between ligand conformations. Resolution
468 of the conformations and the minimal size of the cluster were calculated based on the distribution
469 of the RMSD between ligan conformations. The affinity of ligand binding was estimated by the
470 Autodock program. The pipeline code was deposited to GitHub
471 (github.com/NastiaKozlova/stabilisation complex-receptor-ligand).

472

473 **Acknowledgments**

474 We thank members of the Mitchell Lab for productive discussions. We would like to thank
475 Professor Tracy Raivio (University of Alberta) for the kind gift of pJW15 plasmid. This work was
476 funded by the National Institute of Allergy and Infectious Disease under Award Number R01-

AI155915 (to A.M.M.), the National Institute of General Medical Sciences under Award Number R01-GM121493 (to M.B.), and Texas A&M University start-up funds (to A.M.M.).

Author Contributions: AKR, KS, AK, GCS, MVB, and AMM designed the research. AKR, KS, AK, GCS, and AMM performed the research. AKR, KS, AK, GCS, MVB, and AMM analyzed the data. AKR, KS, AK, GCS, MVB, and AMM wrote the paper.

Competing Interest Statement: The authors declare they have no conflicts of interest.

References

1 Nikaido, H. Molecular basis of bacterial outer membrane permeability revisited. *Microbiology and Molecular Biology Reviews* **67**, 593-656, doi:10.1128/mmbr.67.4.593-656.2003 (2003).

2 Silhavy, T. J., Kahne, D. & Walker, S. The bacterial cell envelope. *Cold Spring Harbor Perspectives in Biology* **2**, doi:10.1101/cshperspect.a000414 (2010).

3 Henderson, J. C. *et al.* The power of asymmetry: Architecture and assembly of the Gram-negative outer membrane lipid bilayer. *Annual Review of Microbiology* **70**, 255-278, doi:10.1146/annurev-micro-102215-095308 (2016).

4 Berry, J., Rajaure, M., Pang, T. & Young, R. The spanin complex is essential for lambda lysis. *J Bacteriol* **194**, 5667-5674, doi:10.1128/jb.01245-12 (2012).

5 Rojas, E. R. *et al.* The outer membrane is an essential load-bearing element in Gram-negative bacteria. *Nature* **559**, 617-621, doi:10.1038/s41586-018-0344-3 (2018).

6 Navarro Llorens, J. M., Tormo, A. & Martinez-Garcia, E. Stationary phase in gram-negative bacteria. *FEMS Microbiol Rev* **34**, 476-495, doi:FMR213 [pii] 10.1111/j.1574-6976.2010.00213.x (2010).

7 Kamio, Y. & Nikaido, H. Outer membrane of *Salmonella typhimurium*: accessibility of phospholipid head groups to phospholipase c and cyanogen bromide activated dextran in the external medium. *Biochemistry* **15**, 2561-2570, doi:10.1021/bi00657a012 (1976).

8 Bogdanov, M. *et al.* Phospholipid distribution in the cytoplasmic membrane of Gram-negative bacteria is highly asymmetric, dynamic, and cell shape-dependent. *Science Advances* **6**, eaaz6333, doi:doi:10.1126/sciadv.aaz6333 (2020).

9 Benn, G. *et al.* Phase separation in the outer membrane of *Escherichia coli*. *Proceedings of the National Academy of Sciences* **118**, e2112237118, doi:doi:10.1073/pnas.2112237118 (2021).

10 Konovalova, A. & Silhavy, T. J. Outer membrane lipoprotein biogenesis: Lol is not the end. *Philosophical Transactions of the Royal Society B: Biological Sciences* **370**, 20150030, doi:doi:10.1098/rstb.2015.0030 (2015).

11 Konovalova, A., Kahne, D. E. & Silhavy, T. J. Outer Membrane Biogenesis. *Annu Rev Microbiol* **71**, 539-556, doi:10.1146/annurev-micro-090816-093754 (2017).

12 Lundstedt, E., Kahne, D. & Ruiz, N. Assembly and maintenance of lipids at the bacterial outer membrane. *Chemical Reviews* **121**, 5098-5123, doi:10.1021/acs.chemrev.0c00587 (2021).

13 John E. Cronan, J. & Rock, C. O. Biosynthesis of membrane lipids. *EcoSal Plus* **3**, doi:doi:10.1128/ecosalplus.3.6.4 (2008).

14 Jones, N. C. & Osborn, M. J. Translocation of phospholipids between the outer and inner membranes of *Salmonella typhimurium*. *Journal of Biological Chemistry* **252**, 7405-7412, doi:https://doi.org/10.1016/S0021-9258(19)66979-6 (1977).

15 Donohue-Rolfe, A. M. & Schaechter, M. Translocation of phospholipids from the inner to the outer membrane of *Escherichia coli*. *Proceedings of the National Academy of Sciences* **77**, 1867-1871, doi:doi:10.1073/pnas.77.4.1867 (1980).

16 Raetz, C. R., Kantor, G. D., Nishijima, M. & Newman, K. F. Cardiolipin accumulation in the inner and outer membranes of *Escherichia coli* mutants defective in phosphatidylserine synthetase. *J Bacteriol* **139**, 544-551, doi:10.1128/jb.139.2.544-551.1979 (1979).

17 Langley, K. E., Hawrot, E. & Kennedy, E. P. Membrane assembly: movement of phosphatidylserine between the cytoplasmic and outer membranes of *Escherichia coli*. *J Bacteriol* **152**, 1033-1041, doi:10.1128/jb.152.3.1033-1041.1982 (1982).

18 White, D. A., Lennarz, W. J. & Schnaitman, C. A. Distribution of lipids in the wall and cytoplasmic membrane subfractions of the cell envelope of *Escherichia coli*. *Journal of Bacteriology* **109**, 686-690, doi:doi:10.1128/jb.109.2.686-690.1972 (1972).

19 Lugtenberg, E. J. J. & Peters, R. Distribution of lipids in cytoplasmic and outer membranes of *Escherichia coli* K12. *Biochimica et Biophysica Acta (BBA) - Lipids and Lipid Metabolism* **441**, 38-47, doi:https://doi.org/10.1016/0005-2760(76)90279-4 (1976).

20 Ishinaga, M., Kanamoto, R. & Kito, M. Distribution of phospholipid molecular species in outer and cytoplasmic membranes of *Escherichia coli*. *The Journal of Biochemistry* **86**, 161-165 (1979).

21 Davydova, L. *et al.* Effects of elevated growth temperature and heat shock on the lipid composition of the inner and outer membranes of *Yersinia pseudotuberculosis*. *Biochimie* **123**, 103-109, doi:https://doi.org/10.1016/j.biochi.2016.02.004 (2016).

22 Osborn, M. J., Gander, J. E., Parisi, E. & Carson, J. Mechanism of Assembly of the Outer Membrane of *Salmonella* typhimurium : Isolation and characterization of cytoplasmic and outer membrane. *Journal of Biological Chemistry* **247**, 3962-3972 (1972).

23 Bogdanov, M. Renovating a double fence with or without notifying the next door and across the street neighbors: why the biogenic cytoplasmic membrane of Gram-negative bacteria display asymmetry? . *Emerging Topics in Life Sciences* **7**, 137-150, doi:10.1042/etls20230042 (2023).

24 Grimm, J. *et al.* The inner membrane protein YhdP modulates the rate of anterograde phospholipid flow in *Escherichia coli*. *Proc Natl Acad Sci U S A* **117**, 26907-26914, doi:10.1101/2020.08.09.213157 (2020).

25 Malinverni, J. C. & Silhavy, T. J. An ABC transport system that maintains lipid asymmetry in the Gram-negative outer membrane. *Proceedings of the National Academy of Sciences* **106**, 8009-8014, doi:10.1073/pnas.0903229106 (2009).

26 Sutterlin, H. A. *et al.* Disruption of lipid homeostasis in the Gram-negative cell envelope activates a novel cell death pathway. *Proceedings of the National Academy of Sciences* **113**, E1565-E1574, doi:10.1073/pnas.1601375113 (2016).

27 May, K. L. & Silhavy, T. J. The *Escherichia coli* phospholipase PldA regulates outer membrane homeostasis via lipid signaling. *mBio* **9**, e00379-00318, doi:doi:10.1128/mBio.00379-18 (2018).

28 Tang, X. *et al.* Structural insights into outer membrane asymmetry maintenance in Gram-negative bacteria by MlaFEDB. *Nat Struct Mol Biol* **28**, 81-91, doi:10.1038/s41594-020-00532-y (2021).

29 Ruiz, N., Davis, R. M. & Kumar, S. YhdP, TamB, and YdbH are redundant but essential for growth and lipid homeostasis of the gram-negative outer membrane. *mBio* **12**, e02714-02721, doi:doi:10.1128/mBio.02714-21 (2021).

30 Douglass, M. V., McLean, A. B. & Trent, M. S. Absence of YhdP, TamB, and YdbH leads to defects in glycerophospholipid transport and cell morphology in Gram-negative bacteria. *PLOS Genetics* **18**, e1010096, doi:10.1371/journal.pgen.1010096 (2022).

31 Jumper, J. *et al.* Highly accurate protein structure prediction with AlphaFold. *Nature* **596**, 583-589, doi:10.1038/s41586-021-03819-2 (2021).
32 Varadi, M. *et al.* AlphaFold Protein Structure Database: massively expanding the structural coverage of protein-sequence space with high-accuracy models. *Nucleic Acids Research* **50**, D439-D444, doi:10.1093/nar/gkab1061 (2021).
33 Josts, I. *et al.* The structure of a conserved domain of TamB reveals a hydrophobic β taco fold. *Structure* **25**, 1898-1906.e1895, doi:https://doi.org/10.1016/j.str.2017.10.002 (2017).
34 Kumar, N. *et al.* VPS13A and VPS13C are lipid transport proteins differentially localized at ER contact sites. *Journal of Cell Biology* **217**, 3625-3639, doi:10.1083/jcb.201807019 (2018).
35 Valverde, D. P. *et al.* ATG2 transports lipids to promote autophagosome biogenesis. *J Cell Biol* **218**, 1787-1798, doi:10.1083/jcb.201811139 (2019).
36 Otomo, T. & Maeda, S. ATG2A transfers lipids between membranes *in vitro*. *Autophagy* **15**, 2031-2032, doi:10.1080/15548627.2019.1659622 (2019).
37 Osawa, T. *et al.* Atg2 mediates direct lipid transfer between membranes for autophagosome formation. *Nat Struct Mol Biol* **26**, 281-288, doi:10.1038/s41594-019-0203-4 (2019).
38 Mitchell, A. M., Wang, W. & Silhavy, T. J. Novel Rpos-dependent mechanisms strengthen the envelope permeability barrier during stationary phase. *J Bacteriol* **199**, e00708-00716, doi:10.1128/JB.00708-16 (2017).
39 Mitchell, A. M., Srikumar, T. & Silhavy, T. J. Cyclic enterobacterial common antigen maintains the outer membrane permeability barrier of *Escherichia coli* in a manner controlled by Yhdp. *mBio* **9**, e01321-01318, doi:10.1128/mBio.01321-18 (2018).
40 Cronan, J. E. The *Escherichia coli* FadR transcription factor: Too much of a good thing? *Mol. Microbiol.* **115**, 1080-1085, doi:https://doi.org/10.1111/mmi.14663 (2021).
41 Nunn, W. D., Giffin, K., Clark, D. & Cronan, J. E. Role for *fadR* in unsaturated fatty acid biosynthesis in *Escherichia coli*. *Journal of Bacteriology* **154**, 554-560, doi:doi:10.1128/jb.154.2.554-560.1983 (1983).
42 Rai, A. K. & Mitchell, A. M. Enterobacterial common antigen: Synthesis and function of an enigmatic molecule. *mBio* **11**, e01914-01920, doi:10.1128/mBio.01914-20 (2020).
43 Paradis-Bleau, C., Kritikos, G., Orlova, K., Typas, A. & Bernhardt, T. G. A genome-wide screen for bacterial envelope biogenesis mutants identifies a novel factor involved in cell wall precursor metabolism. *PLoS Genet* **10**, e1004056 (2014).
44 Ruiz, N., Falcone, B., Kahne, D. & Silhavy, T. J. Chemical conditionality: a genetic strategy to probe organelle assembly. *Cell* **121**, 307-317, doi:10.1016/j.cell.2005.02.014 (2005).
45 Nikaido, H. & Vaara, M. Molecular basis of bacterial outer membrane permeability. *Microbiol Rev* **49**, 1-32 (1985).
46 Bishop, R. E. Structural biology of membrane-intrinsic β-barrel enzymes: Sentinels of the bacterial outer membrane. *Biochimica et Biophysica Acta (BBA) - Biomembranes* **1778**, 1881-1896, doi:https://doi.org/10.1016/j.bbamem.2007.07.021 (2008).
47 Rowlett, V. W. *et al.* Impact of membrane phospholipid slterations in *Escherichia coli* on cellular function and bacterial stress adaptation. *J Bacteriol* **199**, doi:10.1128/jb.00849-16 (2017).
48 Tan, B. K. *et al.* Discovery of a cardiolipin synthase utilizing phosphatidylethanolamine and phosphatidylglycerol as substrates. *Proceedings of the National Academy of Sciences* **109**, 16504-16509, doi:doi:10.1073/pnas.1212797109 (2012).
49 Pluschke, G., Hirota, Y. & Overath, P. Function of phospholipids in *Escherichia coli*. Characterization of a mutant deficient in cardiolipin synthesis. *Journal of Biological Chemistry* **253**, 5048-5055, doi:https://doi.org/10.1016/S0021-9258(17)34655-0 (1978).

50 Nishijima, S. *et al.* Disruption of the *Escherichia coli cls* gene responsible for cardiolipin synthesis. *Journal of Bacteriology* **170**, 775-780, doi:doi:10.1128/jb.170.2.775-780.1988 (1988).
51 Guo, D. & Tropp, B. E. A second *Escherichia coli* protein with CL synthase activity. *Biochimica et Biophysica Acta (BBA) - Molecular and Cell Biology of Lipids* **1483**, 263-274, doi:https://doi.org/10.1016/S1388-1981(99)00193-6 (2000).
52 Kikuchi, S., Shibuya, I. & Matsumoto, K. Viability of an *Escherichia coli pgsA* null mutant lacking detectable phosphatidylglycerol and cardiolipin. *Journal of Bacteriology* **182**, 371-376, doi:10.1128/jb.182.2.371-376.2000 (2000).
53 Suzuki, M., Hara, H. & Matsumoto, K. Envelope disorder of *Escherichia coli* cells lacking phosphatidylglycerol. *Journal of Bacteriology* **184**, 5418-5425, doi:doi:10.1128/JB.184.19.5418-5425.2002 (2002).
54 Shiba, Y. *et al.* Activation of the Rcs signal transduction system is responsible for the thermosensitive growth defect of an *Escherichia coli* mutant lacking phosphatidylglycerol and cardiolipin. *J Bacteriol* **186**, 6526-6535, doi:10.1128/jb.186.19.6526-6535.2004 (2004).
55 Grabowicz, M. & Silhavy, T. J. Redefining the essential trafficking pathway for outer membrane lipoproteins. *Proceedings of the National Academy of Sciences* **114**, 4769-4774, doi:10.1073/pnas.1702248114 (2017).
56 Cronan, J. E., Jr. & Gelmann, E. P. An estimate of the minimum amount of unsaturated fatty acid required for growth of *Escherichia coli*. *J Biol Chem* **248**, 1188-1195 (1973).
57 Feng, Y. & Cronan, J. E. Complex binding of the FabR repressor of bacterial unsaturated fatty acid biosynthesis to its cognate promoters. *Mol. Microbiol.* **80**, 195-218, doi:https://doi.org/10.1111/j.1365-2958.2011.07564.x (2011).
58 Feng, Y. & Cronan, J. E. *Escherichia coli* unsaturated fatty acid synthesis: Complex transcription of the *fabA* gene and *in vivo* identification of the essential reaction catalyzed by FabB. *Journal of Biological Chemistry* **284**, 29526-29535, doi:https://doi.org/10.1074/jbc.M109.023440 (2009).
59 Henry, M. F. & Cronan, J. E. *Escherichia coli* transcription factor that both activates fatty acid synthesis and represses fatty acid degradation. *Journal of Molecular Biology* **222**, 843-849, doi:https://doi.org/10.1016/0022-2836(91)90574-P (1991).
60 Henry, M. F. & Cronan, J. E. A new mechanism of transcriptional regulation: Release of an activator triggered by small molecule binding. *Cell* **70**, 671-679, doi:https://doi.org/10.1016/0092-8674(92)90435-F (1992).
61 Français, M. *et al.* Short-Chain and Unsaturated Fatty Acids Increase Sequentially From the Lag Phase During Cold Growth of *Bacillus cereus*. *Frontiers in Microbiology* **12**, doi:10.3389/fmicb.2021.694757 (2021).
62 Heath, R. J. & Rock, C. O. Roles of the FabA and FabZ β-hydroxyacyl-acyl carrier protein dehydratases in *Escherichia coli* fatty acid biosynthesis. *Journal of Biological Chemistry* **271**, 27795-27801, doi:https://doi.org/10.1074/jbc.271.44.27795 (1996).
63 Lewis, R. N. A. H., Zweytick, D., Pabst, G., Lohner, K. & McElhaney, R. N. Calorimetric, X-Ray Diffraction, and Spectroscopic Studies of the Thermotropic Phase Behavior and Organization of Tetramyristoyl Cardiolipin Membranes. *Biophysical Journal* **92**, 3166-3177, doi:https://doi.org/10.1529/biophysj.106.094003 (2007).
64 Marr, A. G. & Ingraham, J. L. Effect of temperature on the composition of fatty acids in *Escherichia coli*. *Journal of Bacteriology* **84**, 1260-1267, doi:doi:10.1128/jb.84.6.1260-1267.1962 (1962).
65 Garwin, J. L., Klages, A. L. & Cronan, J. E. Beta-ketoacyl-acyl carrier protein synthase II of *Escherichia coli*. Evidence for function in the thermal regulation of fatty acid synthesis.

669 *Journal of Biological Chemistry* **255**, 3263-3265, doi:https://doi.org/10.1016/S0021-
670 9258(19)85692-2 (1980).
671 66 de Mendoza, D., Klages Ulrich, A. & Cronan, J. E. Thermal regulation of membrane fluidity
672 in *Escherichia coli*. Effects of overproduction of beta-ketoacyl-acyl carrier protein synthase
673 I. *Journal of Biological Chemistry* **258**, 2098-2101, doi:https://doi.org/10.1016/S0021-
674 9258(18)32888-6 (1983).
675 67 Knapp, B. D. & Huang, K. C. The effects of temperature on cellular physiology. *Annual*
676 *Review of Biophysics* **51**, 499-526, doi:10.1146/annurev-biophys-112221-074832 (2022).
677 68 Bogdanov, M., Umeda, M. & Dowhan, W. Phospholipid-assisted refolding of an integral
678 membrane protein: Minimum structural features for phosphatidylethanolamine to act as a
679 molecular chaperone. *Journal of Biological Chemistry* **274**, 12339-12345,
680 doi:https://doi.org/10.1074/jbc.274.18.12339 (1999).
681 69 Raetz, C. R. & Whitfield, C. Lipopolysaccharide endotoxins. *Annu Rev Biochem* **71**, 635-
682 700, doi:10.1146/annurev.biochem.71.110601.135414 (2002).
683 70 Conway, T. *et al.* Unprecedented high-resolution view of bacterial operon architecture
684 revealed by RNA sequencing. *mBio* **5**, e01442-01414, doi:doi:10.1128/mBio.01442-14
685 (2014).
686 71 Thomason, M. K. *et al.* Global transcriptional start site mapping using differential RNA
687 sequencing reveals novel antisense rnas in *Escherichia coli*. *Journal of Bacteriology* **197**,
688 18-28, doi:doi:10.1128/JB.02096-14 (2015).
689 72 Adams, P. P. *et al.* Regulatory roles of *Escherichia coli* 5' UTR and ORF-internal RNAs
690 detected by 3' end mapping. *eLife* **10**, e62438, doi:10.7554/eLife.62438 (2021).
691 73 Karp, P. D. *et al.* The EcoCyc database. *EcoSal Plus* **8**, 10.1128/ecosalplus.ESP-0006-
692 2018, doi:10.1128/ecosalplus.ESP-0006-2018 (2018).
693 74 Huerta, A. M. & Collado-Vides, J. Sigma70 promoters in *Escherichia coli*: specific
694 transcription in dense regions of overlapping promoter-like signals. *Journal of Molecular*
695 *Biology* **333**, 261-278, doi:http://dx.doi.org/10.1016/j.jmb.2003.07.017 (2003).
696 75 Mitchell, A. M. & Silhavy, T. J. Envelope stress responses: balancing damage repair and
697 toxicity. *Nature Reviews Microbiology* **17**, 417-428, doi:10.1038/s41579-019-0199-0
698 (2019).
699 76 Szklarczyk, D. *et al.* The STRING database in 2021: customizable protein-protein
700 networks, and functional characterization of user-uploaded gene/measurement sets.
701 *Nucleic Acids Res* **49**, D605-d612, doi:10.1093/nar/gkaa1074 (2021).
702 77 Baba, T. *et al.* Construction of *Escherichia coli* K-12 in-frame, single-gene knockout
703 mutants: the Keio collection. *Mol Syst Biol* **2**, 2006.0008-2006.0008,
704 doi:10.1038/msb4100050 (2006).
705 78 Silhavy, T. J., Berman, M. L. & Enquist, L. W. *Experiments with gene fusions*. (Cold Spring
706 Harbor Laboratory, 1984).
707 79 Datsenko, K. A. & Wanner, B. L. One-step inactivation of chromosomal genes in
708 *Escherichia coli* K-12 using PCR products. *Proceedings of the National Academy of*
709 *Sciences* **97**, 6640-6645, doi:10.1073/pnas.120163297 (2000).
710 80 MacRitchie, D. M., Ward, J. D., Nevesinjac, A. Z. & Raivio, T. L. Activation of the Cpx
711 envelope stress response down-regulates expression of several locus of enterocyte
712 effacement-encoded genes in enteropathogenic *Escherichia coli*. *Infect Immun* **76**, 1465-
713 1475, doi:doi:10.1128/IAI.01265-07 (2008).
714 81 Wong, J. L., Vogt, S. L. & Raivio, T. L. Using reporter genes and the *Escherichia coli* ASKA
715 overexpression library in screens for regulators of the Gram negative envelope stress
716 response. *Methods Mol Biol* **966**, 337-357, doi:10.1007/978-1-62703-245-2_21 (2013).

82 Deatherage, D. E. & Barrick, J. E. Identification of mutations in laboratory-evolved microbes from next-generation sequencing data using breseq. *Methods Mol Biol* **1151**, 165-188, doi:10.1007/978-1-4939-0554-6_12 (2014).

83 Bailey, T. L. & Elkan, C. Fitting a mixture model by expectation maximization to discover motifs in biopolymers. *Proc Int Conf Intell Syst Mol Biol* **2**, 28-36 (1994).

84 Bailey, T. L., Johnson, J., Grant, C. E. & Noble, W. S. The MEME Suite. *Nucleic Acids Res* **43**, W39-49, doi:10.1093/nar/gkv416 (2015).

85 Singer, M. *et al.* A collection of strains containing genetically linked alternating antibiotic resistance elements for genetic mapping of Escherichia coli. *Microbiol Rev* **53**, 1-24 (1989).

86 Rai, A. K., Carr, J. F., Bautista, D. E., Wang, W. & Mitchell, A. M. ElyC and cyclic enterobacterial common antigen regulate synthesis of phosphoglyceride-linked enterobacterial common antigen. *mBio* **12**, e02846-02821, doi:doi:10.1128/mBio.02846-21 (2021).

87 Kim, D., Paggi, J. M., Park, C., Bennett, C. & Salzberg, S. L. Graph-based genome alignment and genotyping with HISAT2 and HISAT-genotype. *Nature Biotechnology* **37**, 907-915, doi:10.1038/s41587-019-0201-4 (2019).

88 Liao, Y., Smyth, G. K. & Shi, W. featureCounts: an efficient general purpose program for assigning sequence reads to genomic features. *Bioinformatics* **30**, 923-930, doi:10.1093/bioinformatics/btt656 (2013).

89 Robinson, M. D., McCarthy, D. J. & Smyth, G. K. edgeR: a Bioconductor package for differential expression analysis of digital gene expression data. *Bioinformatics* **26**, 139-140, doi:10.1093/bioinformatics/btp616 (2009).

90 Ritchie, M. E. *et al.* limma powers differential expression analyses for RNA-sequencing and microarray studies. *Nucleic Acids Research* **43**, e47-e47, doi:10.1093/nar/gkv007 (2015).

91 Bogdanov, M., Sun, J., Kaback, H. R. & Dowhan, W. A Phospholipid Acts as a Chaperone in Assembly of a Membrane Transport Protein. *Journal of Biological Chemistry* **271**, 11615-11618, doi:https://doi.org/10.1074/jbc.271.20.11615 (1996).

92 Sparagna, G. C., Johnson, C. A., McCune, S. A., Moore, R. L. & Murphy, R. C. Quantitation of cardiolipin molecular species in spontaneously hypertensive heart failure rats using electrospray ionization mass spectrometry. *J Lipid Res* **46**, 1196-1204, doi:10.1194/jlr.M500031-JLR200 (2005).

93 Morris, G. M. *et al.* AutoDock4 and AutoDockTools4: Automated docking with selective receptor flexibility. *J Comput Chem* **30**, 2785-2791, doi:10.1002/jcc.21256 (2009).

94 O'Boyle, N. M. *et al.* Open Babel: An open chemical toolbox. *J Cheminform* **3**, 33, doi:10.1186/1758-2946-3-33 (2011).

Figures and Figure Legends

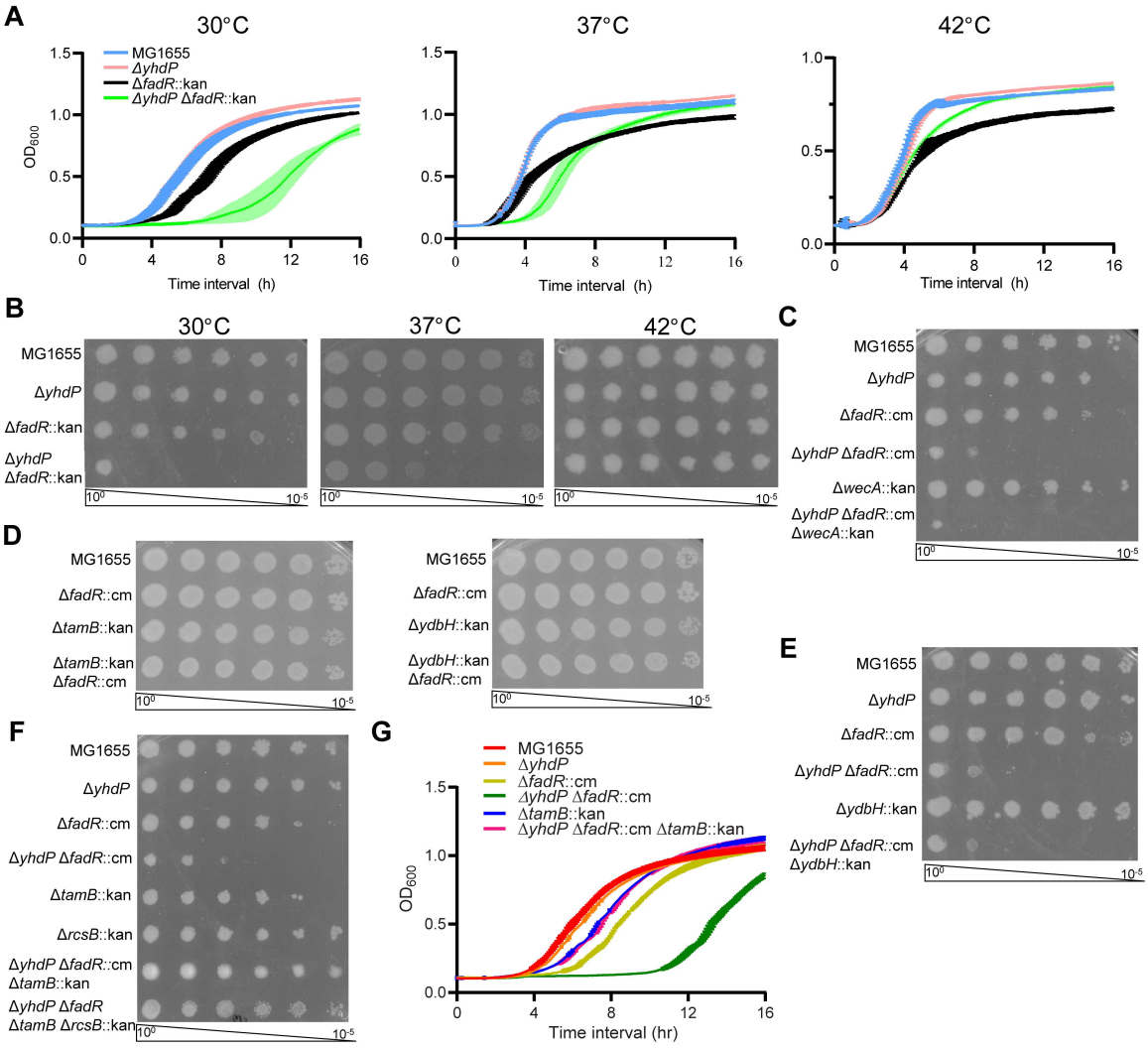

Figure 1. Deletion of *yhdP* and *fadR* causes synthetic cold sensitivity due to impairment of TamB function. (A) The Δ*yhdP* Δ*fadR* strain had impaired growth at lower temperatures. **(B)** EOPs were performed to confirm the growth defect of the Δ*yhdP* Δ*fadR* strain. **(C-F)** EOPs were performed at 30 °C to assess cold sensitivity. **(C)** The growth of the Δ*yhdP* Δ*fadR* strain was not affected by the loss of ECA (Δ*wecA*). **(D)** Neither a Δ*tamB* Δ*fadR* strain nor a Δ*ydbH* Δ*fadR* strain exhibited cold sensitivity. **(E)** Deletion of *ydbH* did not suppress cold sensitivity in the Δ*yhdP* Δ*fadR* strain. **(F)** Deletion of *tamB* completely suppressed cold sensitivity in the Δ*yhdP* Δ*fadR* strain and the Rcs stress response was not necessary for this suppression. **(G)** Growth curves were performed at 30 °C . The Δ*tamB* and the Δ*yhdP* Δ*fadR* Δ*tamB* strain grew equally well, indicating suppression is unlikely to result from slow growth. Quantitative data are shown as the mean of three biological replicates ± the SEM. Images are representative of three independent experiments.

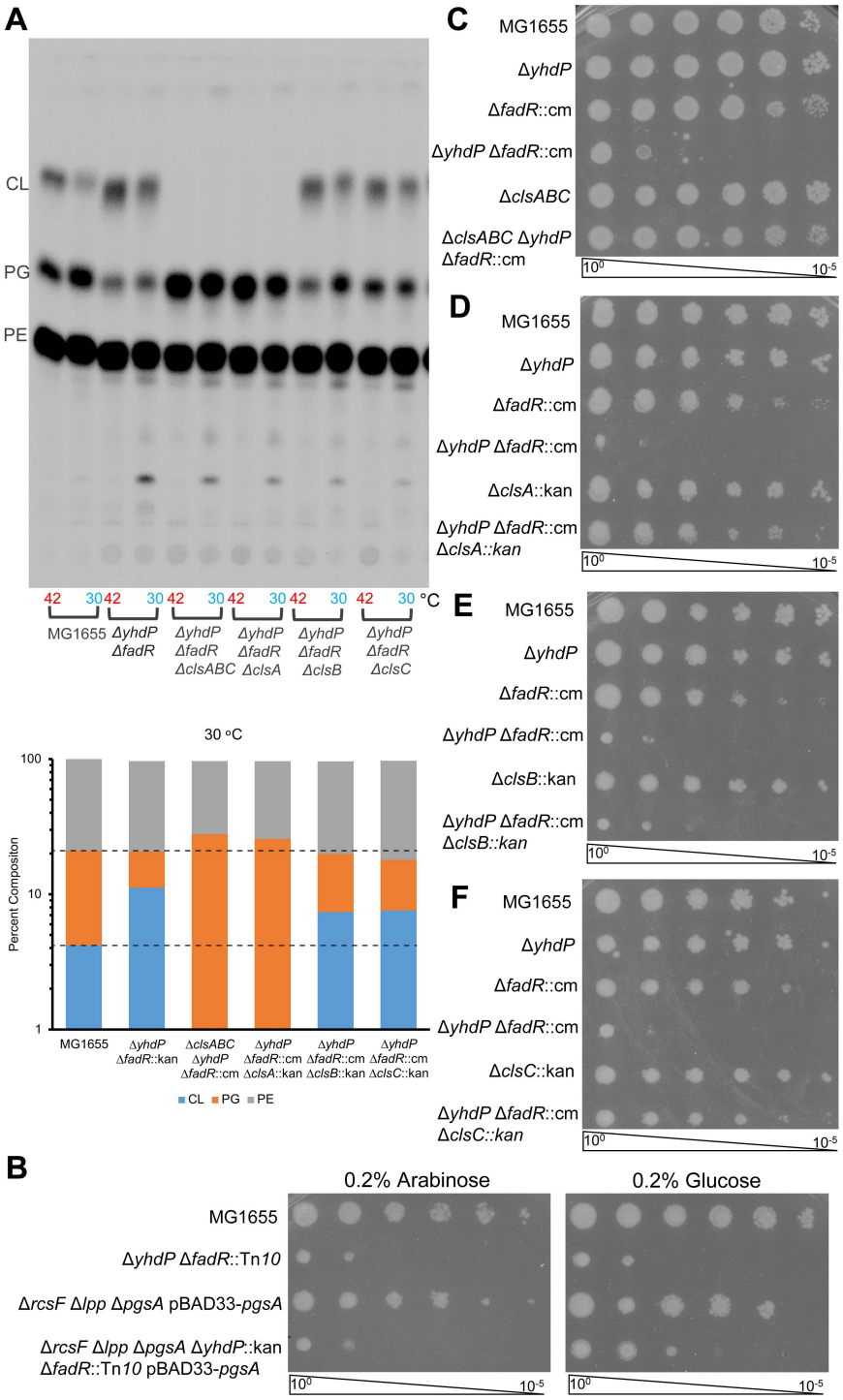

Figure 2. Increased cardiolipin levels are necessary for cold sensitivity of the Δ*yhdP* Δ*fadR* strain. (A) Thin layer chromatography (TLC) of lipid extracts was performed for the indicated cultures grown to OD_{600}=0.2 at 42 °C then transferred to 30 °C or 42 °C for 2 hours before analysis. Relative phospholipid levels are provided for 30 °C samples. The Δ*yhdP* Δ*fadR* strain shows increased levels of CL and a concomitant decrease in PG levels. **(B-F)** Growth effects of

778 altered phospholipid levels were investigated by EOP. Images are representative of three
779 independent experiments. **(B)** PgsA depletion strains in a background where *pgsA* is non-
780 essential were used to assay the effect of lowering PG and CL levels on cold sensitivity. Arabinose
781 induces expression of *pgsA* while glucose represses. Lowering PG and CL levels partially
782 suppressed cold sensitivity. **(C)** Deletion of the three CL synthases, *clsA*, *clsB*, and *clsC*,
783 suppressed cold sensitivity of the Δ*yhdP* Δ*fadR* strain. **(D)** Deletion of *clsA* also suppressed cold
784 sensitivity. **(E)** Deletion of *clsB* does not suppress cold sensitivity, while deletion of *clsC* (F) does.
785

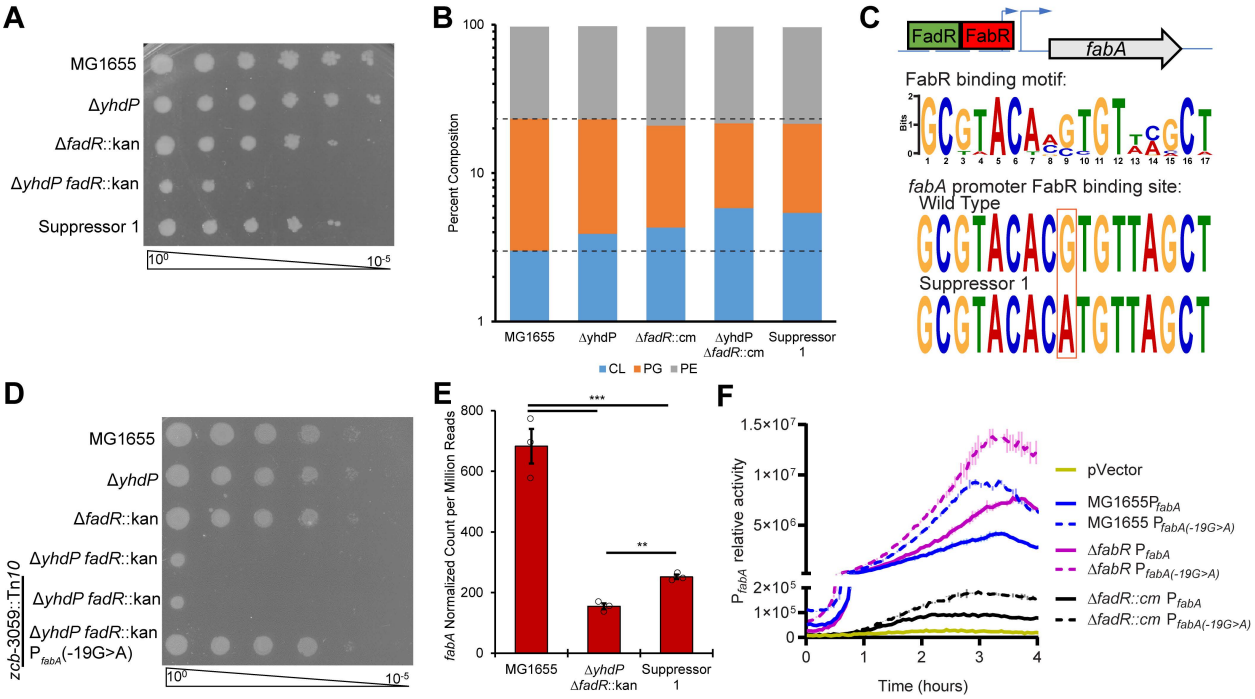

Figure 3. Cold sensitivity can be suppressed by increasing *fabA* expression. (A) The cold sensitivity of a spontaneous suppressor of Δ*yhdP* Δ*fadR* cold sensitivity was tested by EOP. The suppressor returned growth to the level of the Δ*fadR* mutant. **(B)** TLC was performed to assay phospholipid composition. Suppressor 1 showed very similar phospholipid composition to that of its parent strain and did not decrease CL levels. **(C)** A diagram of the promoter region of *fabA* is shown with its transcriptional start sites (blue arrows) and regulator binding sites (boxes). FadR acts as an activator while FabR acts as a repressor. The motif of the FabR binding site, generated using MEME, is shown with the sequences of the parent strain and of Suppressor 1. **(D)** The P_{fabA}(-19G>A) mutation was linked to a Tn*10* and transferred to the Δ*yhdP* Δ*fadR* strain by transduction. The Δ*yhdP* Δ*fadR* strain with P_{fabA}(-19G>A) was not cold sensitivity, confirming suppression. **(E)** *fabA* RNA levels are shown. Bars are the mean of three biological replicates ± the SEM. Individual data points are shown as open circles. ** $p<0.005$, *** $p<0.0005$ by quasi-linear F-test. Data are from the RNA-seq experiment in Figure 5 and *fabA* data are also shown in Figure 5F. **(F)** Luciferase reporters of wild-type and mutant *fabA* promoter activity were constructed. The mutation caused similar fold increases in P_{fabA} activity in all strain backgrounds. Data are luminescence relative to OD_{600} and are shown as the average of two biological replicates ± the SEM.

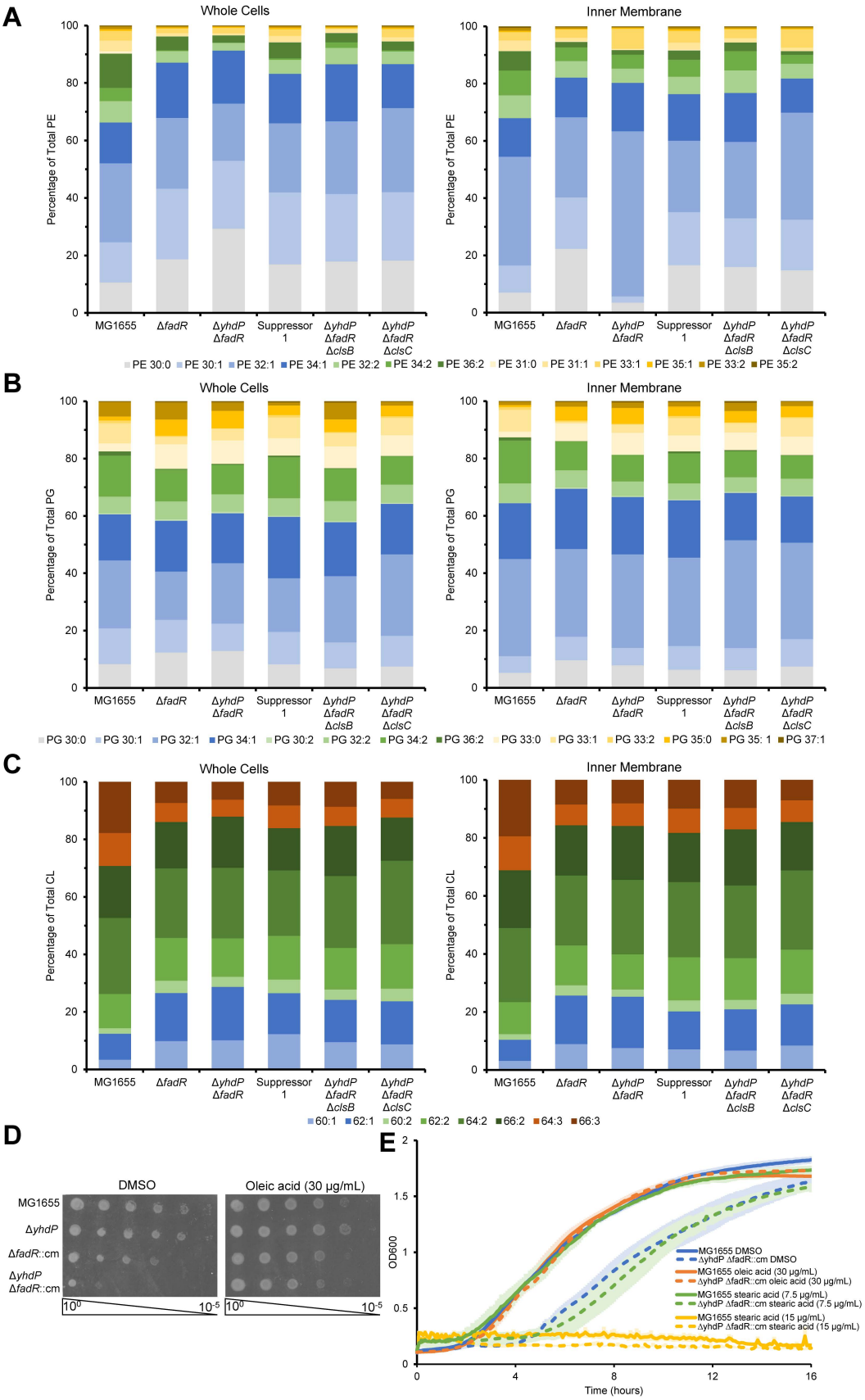
A
Whole Cells
Inner Membrane
Percentage of Total PE
MG1655
ΔfadR
ΔyhdP ΔfadR
Suppressor 1
ΔyhdP ΔfadR ΔclsB
ΔyhdP ΔfadR ΔclsC
PE 30:0 PE 30:1 PE 32:1 PE 34:1 PE 32:2 PE 34:2 PE 36:2 PE 31:0 PE 31:1 PE 33:1 PE 35:1 PE 33:2 PE 35:2
B
Whole Cells
Inner Membrane
Percentage of Total PG
PG 30:0 PG 30:1 PG 32:1 PG 34:1 PG 30:2 PG 32:2 PG 34:2 PG 36:2 PG 33:0 PG 33:1 PG 33:2 PG 35:0 PG 35: 1 PG 37:1
C
Whole Cells
Inner Membrane
Percentage of Total CL
60:1 62:1 60:2 62:2 64:2 66:2 64:3 66:3
D
DMSO
Oleic acid (30 μg/mL)
MG1655
ΔyhdP
ΔfadR::cm
ΔyhdP ΔfadR::cm
10^0
10^-5
E
OD600
Time (hours)
MG1655 DMSO
ΔyhdP ΔfadR::cm DMSO
MG1655 oleic acid (30 μg/mL)
ΔyhdP ΔfadR::cm oleic acid (30 μg/mL)
MG1655 stearic acid (7.5 μg/mL)
ΔyhdP ΔfadR::cm stearic acid (7.5 μg/mL)
MG1655 stearic acid (15 μg/mL)
ΔyhdP ΔfadR::cm stearic acid (15 μg/mL)

807 **Figure 4. Decreasing fatty acid saturation suppresses Δ*yhdP* Δ*fadR* cold sensitivity. (A-C)**
808 Lipid extracts were made from whole cells or from IM separated from OM by differential
809 centrifugation. Strains were grown to OD_{600} 0.2 at 42 °C then shifted to 30 °C for 2 hours before
810 harvest. Lipid extracts were quantified using LC/MS and the percentage of each specific species
811 of PE (A), PG (B), and CL (C) was calculated using the sum of all molecular species detected.
812 Suppressor 1 showed decreased saturation compared to its parent strain (Δ*yhdP* Δ*fadR*). For PE,
813 this difference was evident for whole cells but not for IM. Data for phospholipids without
814 unsaturations are shown in grey, with one unsaturation in blue, with two unsaturations in green,
815 with three unsaturations in orange, and odd chain fatty acids (likely cyclopropyl-fatty acids) in
816 yellow. Data for phospholipids with longer acyl chains are shown in darker colors. **(D)** EOPS were
817 performed on media supplemented with oleic acid or a vehicle control. Oleic acid suppresses the
818 cold sensitivity of the Δ*yhdP* Δ*fadR* strain. **(E)** Growth curves of the indicated strains were
819 performed in the presence of oleic acid, stearic acid, or a vehicle control. Oleic acid suppressed
820 the cold sensitivity of the Δ*yhdP* Δ*fadR* strain while stearic acid did not. Data are the average of
821 three biological replicates ± the SEM.
822

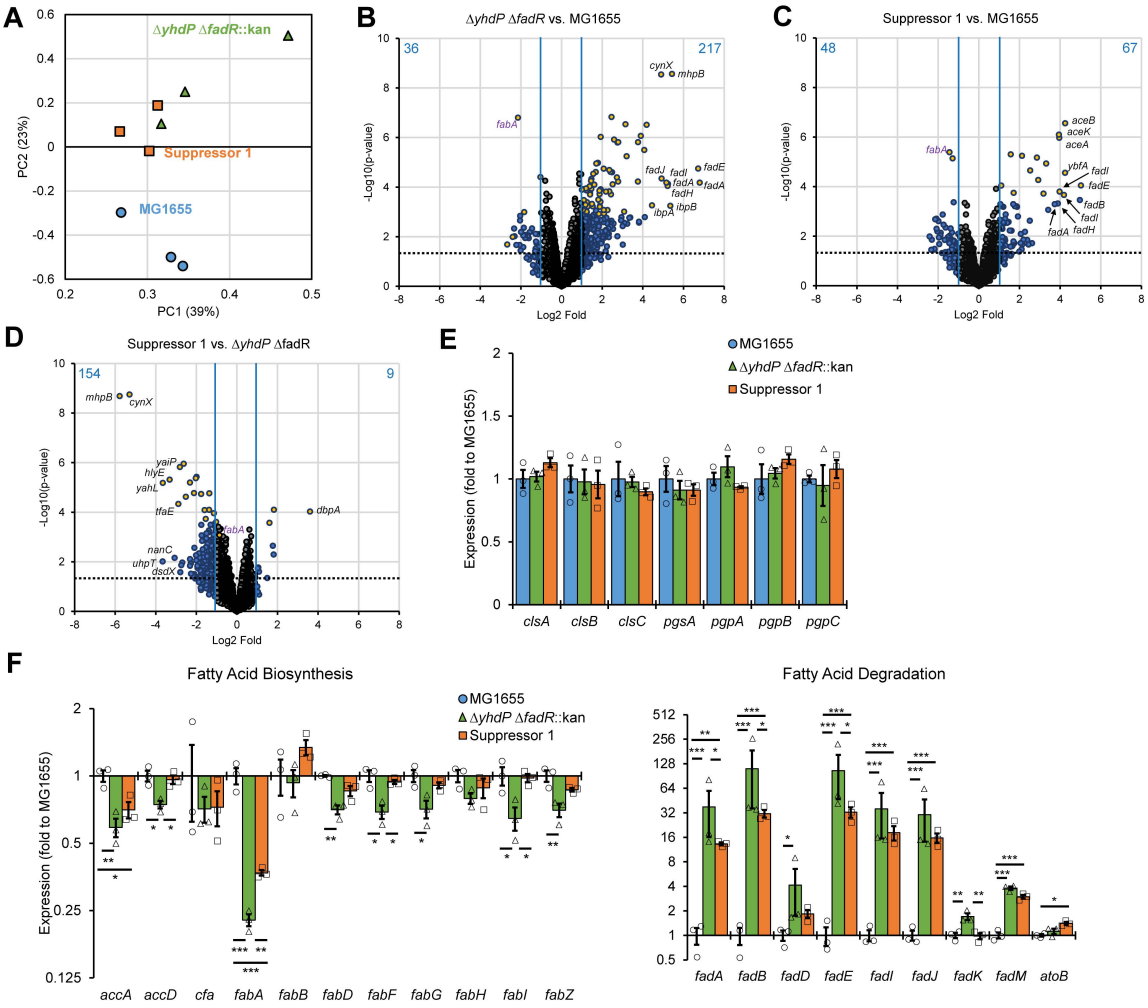

Figure 5. Transcriptional landscape of the Δ*yhdP* Δ*fadR* and suppressed strain. Three biological replicates of the indicated strains were grown at 42 °C to mid-log then transferred to 30 °C for 30 minutes before harvesting RNA and performing RNA-seq. Differential expression was calculated based on a greater than 2-fold change in expression and a p value of less than 0.05 by quasi-linear F-test. **(A)** PCA was performed on the expression of all genes differentially expressed between any groups of samples. Suppressor 1 and the Δ*yhdP* Δ*fadR* strain grouped closer together than to the wild-type strain, although Suppressor 1 was closer to wild type than the Δ*yhdP* Δ*fadR* strain. **(B-D)** Volcano plots show the average fold change and significance of expression changes between the Δ*yhdP* Δ*fadR* strain and wild-type MG1655 (B), Suppressor 1 and wild-type MG1655 (C), and Suppressor 1 and the Δ*yhdP* Δ*fadR* strain (D). Genes with changes greater than 2-fold are shown in blue, while genes with changes less than 2-fold are shown in grey. Genes with a q-value (false discovery rate) of less than 0.05 are shown in yellow. Blue lines indicate a 2-fold change and dotted line indicates p>0.05. The number of up or down regulated genes is indicated in blue. The names of the 10 genes with the largest changes are called out. More genes were up-regulated then down regulated in the Δ*yhdP* Δ*fadR* strain and Suppressor 1 vs. wild type. More genes were down regulated in Suppressor 1 compared to the Δ*yhdP* Δ*fadR* strain. **(E)** Relative expression of genes in the CL synthesis pathway is shown as

841 averages ± the SEM and individual data points. No significant changes were evident. **(F)** Relative
842 expression of genes in the fatty acid synthesis and degradation pathways is shown as averages
843 ± the SEM and individual data points. A general normalizing of these pathways occurred in
844 Suppressor 1 compared to the Δ*yhdP* Δ*fadR* strain; however, the most significant change was in
845 the expression of *fabA*. * $p<0.05$, ** $p<0.005$, *** $p<0.0005$ by quasi-linear F-test.
846

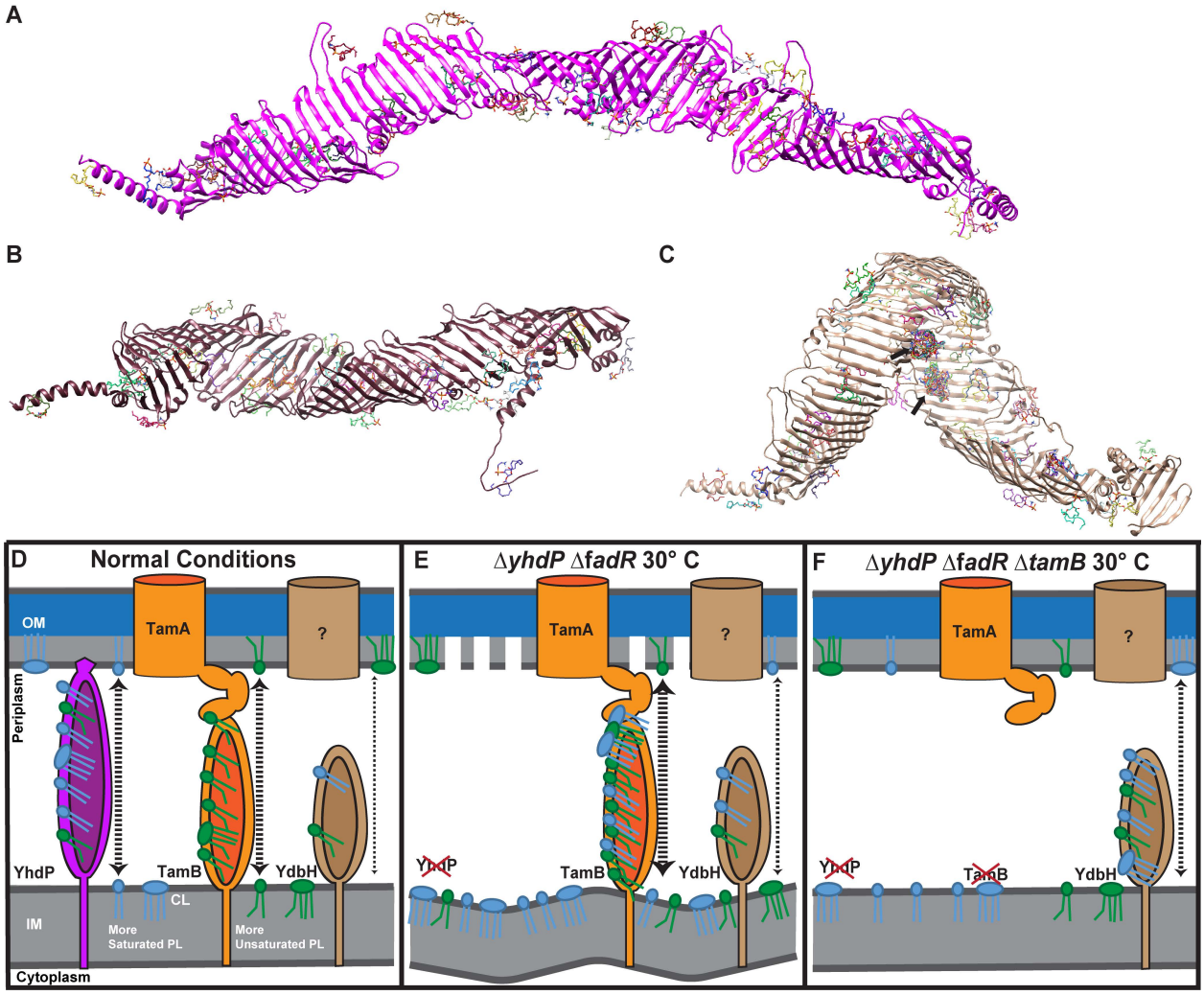

Figure 6. Model for the role of YhdP and TamB in phospholipid transport. (A-C) Docking of short-chain, saturated PE to the predicted structures of YhdP (A), YdbH (B), and TamB (C) was modeled. Conformations of bound PE are shown. Sites where many conformations of PE can bind TamB are indicated with arrows. **(D-F)** Our data can be explained by the following model of phospholipid transport. **(D)** In normal conditions, YhdP is mainly responsible for the transport of phospholipids with more saturated fatty acid chains between the IM and OM. TamB shows a strong preference for transporting phospholipids with more unsaturated fatty acids, with YdbH playing a minor role in phospholipid transport. **(E)** In the Δ*yhdP* Δ*fadR* strain, YhdP is not available to transport more saturated phospholipids and the proportion of both saturated fatty acids and cardiolipin is increased, especially at low temperature. The fluidity of the membrane is also lessened by the low temperature. In these conditions, transport of phospholipids between the membranes is impeded, possibly due to the clogging of TamB by CL or monounsaturated phospholipids. This leads to a lethal lack of phospholipids in the OM and overabundance of phospholipids in the IM. **(F)** When TamB is removed from the Δ*yhdP* Δ*fadR* strain, the clogging

863 of TamB is relieved, and the cell relies on YdbH for phospholipid transport overcoming the cold
864 sensitivity. PL: phospholipid
865